Optimisation of image interpretability and geometric accuracy of airborne videography

Irawan Sumarto

Department of Geodetic Engineering, Institute of Technology Bandung, Email: irawan44@indo.net.id

Abstract

Airborne video images which have several advantages over satellite images and aerial photographs were captured over some selected areas. After they were refined to increase their interpretability, the images were assessed in accordance with the existing map accuracy specifications. Four algorithms of image refinement were tested. These include projective, row duplication, row interpolation and statistical correlation function. Numerous test points were selected on the image and their coordinates were compared to their ground positions. The results suggest that a solid-state video camera can provide images that are sufficiently accurate for medium-scale topographic mapping.

Key words: videography; image refinement and accuracy.

Sari

Ketelitian geometrik dan optimalisasi tingkat ketajaman citra video

Citra video, yang mempunyai beberapa keuntungan dibandingkan dengan citra satelit dan foto udara, diperoleh dari hasil penerbangan di atas suatu daerah. Setelah citra tersebut direstorasi untuk meningkatkan tingkat ketajamannya, dilakukan proses fotogrametri untuk mengevaluasi tingkat ketelitian geometriknya. Restorasi citra dilakukan secara digital dengan empat macam teknik, yaitu projektif, interpolasi baris, dupikasi baris, dan korelasi statistik. Evaluasi ketelitian geometrik dilakukan dengan membandingkan koordinat sejumlah titik yang diamati pada citra video dengan posisi seharusnya di lapangan. Hasil pengujian mengindikasikan bahwa kamera video dapat digunakan pada pemotretan udara bagi keperluan pemetaan topografi skala menengah.

Kata kunci: videografi, pemulihan dan ketelitian geometrik citra video.

1 Introduction

The two most common sources of digital images used for mapping purposes are satellite scanners and scanned aerial photographs. These images provide a wide ground coverage and a high metric stability. However, they have some limitations, e.g. the geometric resolution of satellite images is not adequate for large and medium scale mapping (Steiner, 1992). Also, the price of the images can be prohibitive for some users and the delivery time is slow. Likewise, scanned aerial photographs are not always a cost-effective source of imagery since the purchase of a sophisticated photogrammetric scanner is not always affordable, and scanning services are expensive and often not readily available. Further, satellite orbits are pre-programmed to cover a particular area only at certain times (Jensen, 1986) and cloud coverage is always a problem in some parts of the world (Torlegard, 1992). Neither of these acquisition techniques is suitable for the low-cost, continuous and real-time topographic mapping activity.

Hence, an alternative source of digital topographic images is an attractive option. This paper examined the prospects of using a video camera for topographic mapping by evaluating the positional accuracy achieved.

2 Airborne videography

Airborne videography is emerging as a cost-effective remote sensing tool for use by resource managers (Repic et al, 1991). Several interesting characteristics of videography are mentioned by Wright (1993). They are the general availability, portability, simplicity and low cost aspects of the equipment which provides a great amount of data for processing in real time and in softcopy form. The system also has a wide spectral sensitivity. These characteristics have promoted an increase in the use of airborne videography for aerial surveying and, over the past ten years, it has become

widely used for image interpretation (Richardson et al, 1985; Everitt et al, 1988; Vlcek, 1988).

When all the variables involved in the imaging technique are considered, video images are found to be less accurate than aerial photography of the same scale. One image frame from a video camera is made up of odd and even fields taken consecutively at one-fiftieth of a second interval. In conventional use the consecutive odd and even images are assumed to be taken simultaneously from the same position. This assumption cannot be made for airborne platforms where the movement of the camera introduces a significant shift between the two fields. The clarity of terrain features is reduced following image composition of both fields into one full frame.

To replicate the normal coverage of a still camera, and to increase the interpretability of the images, consecutive odd and even fields of a video frame must be restored into a composite interpretable frame. Several techniques have been proposed to improve the quality of the composite image (Sumarto, 1997). They include the use of correlation functions, projective transformation, row duplication and row interpolation or averaging.

3 Experiments

Aerial frames were collected and processed via conventional mapping orientation on a digital photogrammetric workstation. The collected video frames were then pre-processed by the four algorithms to improve their interpretability. A number of pre-defined check points were also coordinated. The positional accuracy was checked by comparing the data derived from video with independent reference data collected in large scale aerial imagery and known to be at least ten times more accurate.

3.1 Study area

The campus of Curtin University of Technology was selected as a study area. This area is located at Bentley in the City of Canning, Perth, Western Australia. It encompasses various types of terrain reflecting the average conditions of local urban areas, where low-rise buildings, road networks, and green belts are characteristic features. Topographic elevations vary from 6 m to 20 m above the Australia geodetic datum (AGD) and buildings range from one to six levels in height. It was considered an ideal testing area for airborne videography.

Numerous ground control points which could be used as control or check points were available within the area. Wide angle aerial photographs at a scale of 1:4,000 and flown in 1991 were also available. Film positives of the

large scale images were used to densify the ground control and provide the check points necessary for this research.

Several missions were flown at approximately 500 m above the National datum, giving a choice of overlap and scene illumination. At this height the image scale was approximately 1:65,000 and the ground coverage of a single image was approximately 300 m by 400 m.

3.2 Image interpretability

Image interpretability means the degree to which objects in the image can be clearly recognised. A sharp image provides more accurate information and is easier to interpret. Many factors influence the quality of the images, most significant of which is lens quality. Other factors, such as image motion effect and the nature of the video imaging processes, also affect the level of interpretability.

Video images taken from a moving platform suffer from motion distortion which degrades the sharpness of the image. The most obvious effect of motion is the blur that occurs when the sensor moves relative to the target during the imaging process. This effect, however, can be reduced by using a high speed shutter (when available), or by mounting the video camera in the aircraft so that the scanning direction is parallel but opposite to the flight direction (Pickup et al, 1995).

Other significant distortions that reduce the interpretability of an airborne video image occur because the present video cameras operate in an interlaced mode. The odd and even fields are collected consecutively. When the video camera is moving, the second field is taken from a slightly different position resulting in a double image effect. Figure 1 clearly shows the effect of interlacing on an airborne video image. The objects are deformed in a systematic pattern where every second row is horizontally displaced relative to the next contiguous row. The forward motion of the aircraft causes the deformation.
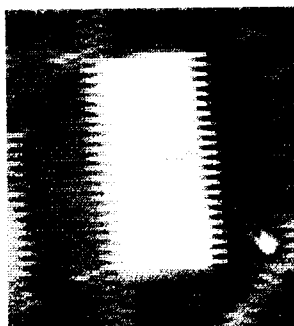

Figure 1 Systematically deformed objects caused by the movement in the video imaging system platform

A further problem is the displacement caused by aircraft pitch, yaw and roll which can be as great as the forward motion effect but not systematic from one frame to the next. This means that adjacent features are no longer adjacent in the image.

The determination of field displacement or the geometric correction of the image is a rather complex task. If the aircraft speed, attitude and altitude during imaging are recorded accurately, field displacement can be calculated. However, this solution is rarely found to be practical. It is usually necessary to determine relative shifts in the odd and even field locations using other techniques. These are outlined in the following section.

4   Refinement of video images

Several algorithms for image refinement have been used in this research. The algorithms include:

- statistical auto-correlation function (SCF or ACF),
- projective transformation,
- row duplication and,
- row interpolation.

4.1   Statistical correlation function

A correlative procedure is another method for determining the relative vertical and horizontal displacement between the fields within a frame regardless of camera orientation. Computation of these statistical properties of the image was adopted by Pickup et al (1995). The statistical properties of the image are used to calculate the relative displacement between the odd and even fields within a frame and this shift is then used to refine the image. This method is based on statistical correlation theory where the correlation value will be high when there is a strong correlation between both fields, and will decrease as row and column displacement increases.

For an ideal frame, where there is no lateral nor longitudinal shift between fields, the correlation function between the odd and even fields will peak when the lag equals zero (l=0) and gradually decline as the lag increases. The deviation from expected values can be used to estimate the amount of displacement in both the vertical and horizontal directions of a field. However, when the cross-correlation peaks at a horizontal and/or a vertical spatial lag different from zero, then that lag describes the amount of field displacement and the shift necessary to restore the geometric properties of the image.

This method computes the correlation between two fields of a frame. A single correlation between each column and row in the even and odd fields is computed for the whole image frame. High correlation will occur

when two columns or rows are identical or similar. The location corresponding to the highest correlation coefficient then represents the necessary column or row shift between both fields.

Once the amount of pixel shift had been determined, the image is refined by applying the nearest integer shift in the grey-value of every pixel on all the even rows (even field), along the row itself. In this manner the original image shown in Figure 1 can be reconstructed as shown in Figure 2a, which exhibits better interpretability.
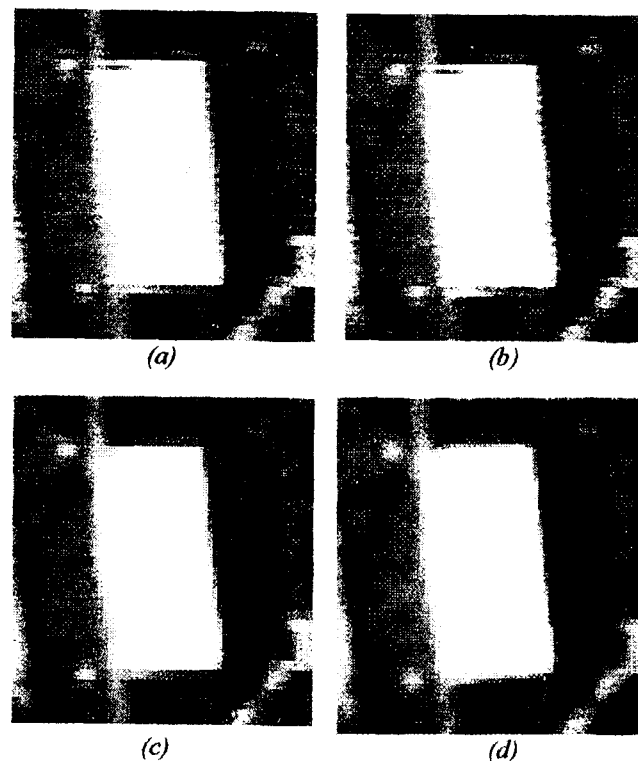

(a) *(b)*

(c) *(d)*

Figure 2   Video images after refinement using (a) SCF method, (b) Projective, (c) Duplication, (d) Averaging

4.2   Projective transformation

Projective geometry in photogrammetry deals with the geometric characteristics of projectively related features. An aerial video image is a projection of objects on the ground, so they are, at the moment of exposure, projectively related. This relationship can, ideally, be determined by a space resection which is a rigorous three-dimensional projective transformation. The transformation parameters describe the location and orientation of the aerial camera. These values can then be used to transform photo coordinates to the ground system or vice-versa.

The space relationship between the even and odd fields in a frame, however, can be adequately determined using a two dimensional projective transformation because of the identical surface model for each image. The two dimensional projective transformation equations (Equation 1) is used in the analytical

computation of the two dimensional image coordinates of points after they have been projected into a plane from another non-parallel plane (Figure 3). The positions of points on a plane can be related to their corresponding projected positions on another plane or, in this case, coordinate positions of points on the even field can be projectively related to their corresponding positions on the odd field. When all the necessary parameters relating to both fields are known, all the information in the one field can be transformed into the other.

$$\begin{bmatrix} x \\ y \end{bmatrix} = \begin{bmatrix} x & 0 & y & 0 & 1 & 0 & xx' & yx' \\ 0 & x & 0 & y & 0 & 1 & xy' & yy' \end{bmatrix} \begin{bmatrix} a_1 \\ a_2 \\ b_1 \\ b_2 \\ c_1 \\ c_2 \\ a_0 \\ b_0 \end{bmatrix} \qquad (1)$$

where   x,y = coordinates in system 1,
        x', y' = coordinates in system 2,
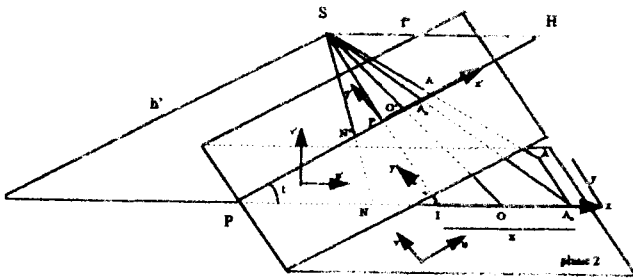   ai,bi,ci = transformation parameters.

Figure 3 Projective relationship

4.2.1 Video image refinement

Field displacement in a field image can be eliminated by transforming the plane of the even into that of the odd field using a projective transformation. An indirect transformation was used to restore the image in this study. During the pixel transformation, the relative pixel shift between the two fields is eliminated resulting in a reconstructed image which is theoretically free from relative field displacement. A grey-value for the transformed pixel was then interpolated using the nearest-neighbour method principally to maintain the overall image integrity and not introduce new brightness values or digital numbers (DN). Figure 2b shows an example of an image refined by this method.

4.3 Estimation by neighbouring row duplication

In remote sensing a cosmetic operation is usually applied to reconstruct digital images which contain either partially or entirely missing scan rows caused by a

tion in the sensor or other components of the scanner. An estimate of what the original values might have been may be made by considering values in the rows adjacent to the missing rows (Mather, 1987).

There are three ways of achieving this: neighbour row replacement, adjacent row interpolation or reconstruction using information from two adjacent bands (Bernstein et al, 1984; Fusco and Trevese, 1985). However, the third method was not implemented in this study as video image has only one band.

The first method estimates the missing pixel value from the value of the corresponding pixel in the closest preceding row. For example, if the missing pixel value is denoted by v_{ij} (pixel i in row j) then the formula is:

$$v_{ij} = v_{ij-1} \qquad (2)$$

For the case when the missing row is the first of an image then the second row can be copied. However, this method will introduce an image defect particularly in linear features. When the feature is nearly parallel to the missing row, a double image will occur. Moreover, copying a row increases pixel resolution in one direction and will affect the aspect ratio of the image. Figure 2c shows an example of image refined using this technique.

4.4 Estimation by adjacent row interpolation

The second method uses DN from adjacent rows; the rows above and below the missing row. The DN for each pixel on the row is computed by averaging corresponding pixel values on the adjacent rows.

$$v_{ij} = \text{Int} \{ (v_{ij-1} + v_{ij+1})/2 \} \qquad (3)$$

This method may produce a new DN in a row which is not typical of those in neighbouring rows. This can happen when the missing row coincides with the border of two distinct features, such as the border between land and water. The interpretability of the image is improved if a feature is nearly vertical.

In the case of a straight diagonal line or one nearly horizontal, the refined image may exhibit a stair pattern or the line may split, thereby degrading image quality (Fusco and Trevese, 1985). Figure 2d shows an image refined using this technique

5   Criteria for assessment of interpretability

Assessment of the resampled images may best be made by visual examination of vertical features as shown in Figures 2a, b, c, d. All images show an improvement in clarity. They look sharper than the original images (Figure 1). However, to evaluate the improvement in interpretability, it is necessary to define quantitative

criteria and develop procedures which will allow an objective comparison of the various methods of image refinement. To avoid judgement based only on a subjective or personal view of the interpretability, a method of statistical assessment has been proposed and described.

The proposed two statistical methods compare the refined image with the expected frame or a control frame. The statistical properties of the images are used to assess similarity. The cross-correlation coefficient (() between the two images reflects the level of similarity. Values near to one (1) indicate images that are strongly correlated and contain nearly the same information (grey-values). Any deviation from one means the image is less correlated and when the coefficient is equal to zero there is no correlation. Secondly, the root mean square (RMS) of ratioed image also reflects the level of similarity between the refined and control images. High similarity is found when the value is close to zero.

A scanned aerial photograph covering the same area was used as the control frame (Figure 4). The photograph was preferred to a simulated image because it was subject to a similar error budget to the video image, except for the line interlacing effect. Unfortunately the photograph was not taken simultaneously with the video images, so factors such as weather, sun angle, and camera tilt may have had some small differential effect on the DN of similar features. Consequently a strong correlation between the scanned photograph and refined video images was not expected in this test.
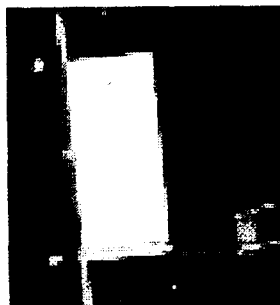

Figure 4 Scanned aerial photograph

5.1 Numerical assessment by statistical methods

Images that contain similar or identical information, in statistical terms, are strongly correlated. For example, due to the spectral characteristics of vegetation, multi-spectral images of vegetated areas have a positive correlation amongst the visible bands and a negative correlation (un-correlated) between near-infrared and visible red bands. The presence of a positive correlation implies that some information contained on the images was similar and the correlation coefficient reflects the

level of similarity or repetition of information between the images.

In the first strategy applied in this research, correlation coefficients were computed for all four refined images with respect to the true or control image. As was explained, a scanned aerial photograph (Figure 4) covering the same area, was assumed to be a true image and used as the control image. The computed coefficients reflect the degree of similarity between each of the refined images and the control image. A higher coefficient indicates a refined image which is more comparable with the sharp, clear, control image and therefore likely to be more interpretable.

Image to image transformations were performed in order to minimise origin and orientation differences between refined and control images. Image re-sizing was also necessary to overcome small-scale differences. The four refined images, SCF, projective, line duplication, and averaging interpolation along with the unrefined image were then compared with the control image.

Two areas occupying nominally 4000 and 30,000 pixels were extracted from each of the images. The large number of points in each area was sufficient for statistical analysis and demonstration of the different performance of reconstruction algorithms on different image patterns. Correlation coefficients between the control and the aforementioned five images were then computed. The results are summarised in Table 1.

Table 1 Percentage correlation coefficients of area 1 and 2 relative to the control image

Area \ Image	A	B	C	D	E
1	53.42	54.47	54.64	54.49	**54.98**
2	56.59	**65.86**	65.86	65.66	65.53

The second strategy for statistical analysis involved the computation of ratioed images. The reference image was divided first by the original unrefined image and then each of the four refined images. Theoretically, if both images involved in the ratio were identical, the new ratioed image would consist of an array of pixel elements all equal to one. Any deviation from one would indicate difference between images. The root mean square (RMS) difference of pixel values in the ratioed images computed using Equation 4 reflected these differences. Smaller RMS values indicated closeness of the refined images to the standard image. The results are summarised in Table 2.

$$RMS_{diff} = \sqrt{\frac{1}{n}\sum_{i=1}^{i=n}(E_i - \bar{E})^2} \qquad (4)$$

where $\bar{E}$ = mean value of pixel ratio,
        n = number of pixels,
        E_i = value of pixel ratio i.

Table 2 Root mean square (RMS) values of ratioed image of window 1 and 2

Area Image	A	B	C	D	E
1	0.833	0.820	0.820	0.823	**0.803**
2	0.810	0.794	0.794	0.796	**0.743**

5.2 Results and discussion

Because the analogue based reference image was captured at a different time to the digital video images, minor temporal radiometric and optically caused geometric differences existed Perfect correlation was not anticipated (Table 1). The results, however, indicate that there was an improvement in the quality of images after reconstruction by particular algorithms. Results obtained by using the different algorithms have been ranked

All methods produced significant improvement as the correlation coefficients increased and RMS errors decreased. Statistics show that all the refined images show improvement which peaked at 16 percent for correlation coefficients (Table 1) and eight percent for rationing (Table 2). Although marginal, there was clear statistical evidence that the row interpolation algorithm produced superior results.

The results indicate that line replication performed worst. The SCF and projective transformation algorithms were slightly better. More significant improvements were obtained by using the averaging or row interpolation approaches. The statistical data indicate that this method increased the image interpretability by approximately eight percent when compared with other methods.

6 Geometric assessment

It should be stressed that for low-order applications, such as local map updating, aerial triangulation is not a primary concern because accurate ground control can usually be extracted from available large scale maps or aerial photographs. For this research existing 1:4,000 aerial film positives were measured in a precise analytical stereo digitiser.

In total there were more than 80 points measured on a Wild BC-2 analytical stereo digitiser and used for control or check points. The points were large, natural or artificial features which could easily be recognised. They included the corners of buildings, a chimney, a road junction, a street island, a manhole and parking lines

The RMSE of photogrammetrically derived coordinates taken from the large scale photographs for control and check points was considered very low compared to the

errors in the coordinates extracted from the video images. The scale of the video image was much smaller (about 17 times) than the scale of aerial photographs. Therefore in the error propagation chain, the video image error was overwhelming (Ding, 1996).

6.1 Geometric accuracy

The accuracy of measurements from photographs can be classified either as absolute or relative (Warner, 1989; 1990). Absolute accuracy is the exactness in the location of a given point on the image compared with its true position. It is usually given in standard x, y and z coordinates. Relative accuracy refers to the location of different points relative to each other.

Photogrammetrists have always been concerned about the accuracy of their observations and products. GIS managers require absolute accuracy so that new data can be integrated into existing databases without ambiguity. Map overlays, intersections or analyses cannot be performed if the data are inaccurate (Thapa and Bossler, 1992). Relative accuracy, on the other hand, is of interest to map users, such as planners or resource managers, who usually want to measure distances and height differences between points.

Both the relative and absolute accuracies of measurements made in this research were computed. Absolute accuracy is represented by the root mean square (RMS) of the discrepancy in coordinates computed using Equation 5. Relative accuracy is represented by the RMS of discrepancy in distances or heights measured at check points computed using Equation 6.

$$RMS_{disp} = \sqrt{\frac{1}{n}\sum_{i=1}^{i=n}(x_{obs_i} - x_{gcp_i})^2} \qquad (5)$$

$$RMS_{disp} = \sqrt{\frac{1}{n}\sum_{i=1}^{i=n}(d_{obs_i} - d_{gcp_i})^2} \qquad (6)$$

6.2 Restitution of stereomodels and point measurement

After performing an individual image refinement aimed at optimising interpretability, stereomodels were oriented on an Intergraph ImageStation softcopy photogrammetric workstation using a minimum of twelve points for relative orientation and six points for absolute orientation. Computed lens and camera parameters were included in this process. Image differential scale and lack of orthogonality were compensated during interior orientation. The results of the absolute orientation (AO), in particular the RMS of the ground control coordinate residuals, are presented in Table 3.

With 70 percent forward overlap and 1:65,000 image scale, one stereomodel covers approximately 300 m by 300 m on the ground. This area is less than one percent of the area of a stereo model generated from full format image at the same scale. Base-to-height ratio of the model was 0.3 which is half that for 60 percent overlapping wide angle imagery.

Stereoscopic observations were made on pre-selected check points. An estimation of absolute accuracy, as indicated by the RMS of coordinate discrepancies, was computed and the results are summarised in Table 3.

More than 50 distances and height differences were also measured in each stereomodel. These measurements were then compared with the corresponding ground distances measured on the large format as control images. The RMS of discrepancy of the measurements are presented in Table 4.

6.3 Discussion

Table 3 presents the model configuration for stereo restitution and estimates of the accuracy of absolute orientation based on stereo measurement residuals on ground control and check points. These values collectively indicate the accuracy of point measurement in the stereoscopic video images.

The internal accuracy, resulting from the absolute orientation of the stereomodels, was predictably lower than for equivalent scanned aerial images. The RMS of the coordinate residuals at the control points were respectively 0.866 m and 0.873 m for planimetry and height. External accuracy or RMS of residuals at check points for planimetric and height was about 1.5 m.

The RMS of residuals at check points were S_{xy} = 1.303 m and S_z = 1.544 m, about 1.6 times larger than the control points. It can be seen that the horizontal accuracy was better than the height accuracy. This was mainly due to the weak base-to-height ratio of the video stereomodels.

Table 3 RMS of discrepancy at control and check points

Model No.	Scale	B/H	No. GCP Check	RMS at control points x y xy(m)	RMS at control points h (m)	RMS at check points x y xy(m)	RMS at check points h (m)
1	1:66323	0.29	7 18	0.748 0.489 0.894 (13.4*)	0.995	0.570 0.840 1.040 (15.7*)	1.813
2	1:66146	0.29	8 41	0.664 0.337 0.745 (11.3*)	0.978	0.824 0.927 1.240 (18.7*)	1.278
3	1:63716	0.39	7 8	0.729 0.634 0.960 (15.1*)	0.645	1.136 1.169 1.631 (25.6*)	1.540
			Average	0.866	0.873	1.303	1.544

*at image scale (μm)

Table 4 Relative accuracy of horizontal distances and height differences

Model No.	Scale	B/H	N	Relative Accuracy RMS Dist. (m)	Relative Accuracy RMS ΔH(m)
1	1:66323	0.29	≈ 50	0.815 (12.3*)	1.221
2	1:66146	0.29	≈ 80	1.146 (17.3*)	1.296
3	1:63716	0.39	≈ 50	1.277 (20.0*)	1.333
			Average	1.079	1.2283

*at image scale (μm)

Although the check point RMSE equated to 23 (m on the 1.65.000 video image (approximately three pixels), the results were of sufficient quality to meet user specifications for maps at a scale of 1:15.000 or smaller (DOLA. 1994) or for maps at a scale of 1:25,000 (Bakosurtanal, 1992).

Table 4 display the relative accuracy of distances and heights measured on the video image, compared with those measured on the large format control images. The RMS of the discrepancies in distance and height differences were found to be slightly larger than one metre, specifically 1.079 m for horizontal distances and 1.283 m for height differences. With respect to the longest distance used in the stereomodel, some 230 m, this represented a relative accuracy which is about 0.5 percent or 1/200.

7   Conclusions

The intention of this study was to provide evidence that airborne video images could be used for mapping purposes where only moderate accuracy is required. Considering the error chain involved in analogue video imaging, it was understood that standard aerial photographs would be still the primary mapping image with the video image having a minor revision role. This preliminary investigation has demonstrated that it is feasible to employ a video camcorder in aerial mapping for applications which require low order accuracy.

The reconstruction of airborne video images by all four methods produced a better quality image. Qualitative observation of all the refined images showed that they were sharper and more easily interpreted than the original non-refined image. Additional results from a quantitative statistical analysis also indicated that all methods improved the image. The row interpolation method was superior to the others. It can be concluded that, by using this interpolation method, defects in an airborne video image caused by platform motion can be refined so as to produce a reconstructed image of adequate quality for ortho-image production.

The work carried out has indicated the potential of a video camcorder to supply aerial images for application such as local medium scale mapping or map revision programs. The attainable accuracy is around 1.5 m when flying from minimum altitudes and using wide angle lenses. This accuracy will meet user specification for map revision at scales of 1:15,000 or smaller.

8   References

1. Bakosurtanal (1992) Spesifikasi Peta Rupabumi Indonesia Skala 1:25,000, National Map Specification, Cibinong, Indonesia.

2. Bernstein, R., Lotspiech, J.B., Myers, J.H., Kolsky, H.G., and Lee, R. (1984) Analysis and Processing of LANDSAT-4 Sensor Data Using Advanced Image Processing Techniques and Technologies, Institute of Electrical and Electronic Engineers Transactions on Geoscience and Remote Sensing, Vol. GE-22, No. 3, pp. 192-221.

3. Ding, X. (1996) Personal Communication, Department of Land Surveying and Geo-Informatics, Hong Kong Polytechnic University,Hung Hom, Kowloon, Hong Kong.

4. Department of Land and Administration (DOLA) (1994) Topographic Data Acquisition, Standard Specification Circular, Department of Land Administration, Perth, Australia.

5. Everitt, J.H., Escobar, D.E., Gerbermann, A.H. and Alaniz, M.A. (1988) Detecting Saline Soils with Video Imagery, Photogrammetric Engineering and Remote Sensing, Vol. 54, No. 9, pp. 1283-1287.

6. Fusco, L. and Trevese, D. (1985) On the Reconstruction of Lost Data in Images of More than One Band, International Journal of Remote Sensing, Vol. 6, No. 9, pp. 1535-1544.

7. Jensen, J.R. (1986) Introductory Digital Image Processing: A Remote Sensing Perspective, Prentice Hall, New Jersey, USA, 379 pp.

8. Mather, P.M. (1987) Computer Processing of Remotely-sensed Images: An Introduction, John Wiley and Sons, Suffolk, UK, 352 pp.

9. Pickup, G., Chewings, V.H. and Pearce, G. (1995) Procedures for Correcting High Resolution Airborne Video Imagery, International Journal of Remote Sensing, Vol. 16, No. 9, pp. 1647-1662.

10. Repic, R.L., Lee, J.K. and Mausel, P.W. (1991) An Analysis of Selected Water Parameters in Surface Coal Mines Using Multispectral Videography, Photogrammetric Engineering and Remote Sensing, Vol. 57, No. 12, pp. 1589-1596.

11. Richardson, A.J., Menges, R.M. and Nixon, P.R. (1985) Distinguishing Weed from Crop Plants Using Video Remote Sensing, Photogrammetric Engineering and Remote Sensing, Vol. 51, No. 11, pp. 1785-1790.

12. Steiner, D.R. (1992) The Integration of Digital Orthophotographs with GIS in a Microcomputer Environment, ITC Journal, Vol. 1992-1, pp. 65-72.

13. Sumarto, I (1997) An Investigation into the Applicability of Airborne Videography for Topographic Mapping, Unpublished Ph.D Thesis, Curtin University of Technology, Perth, Western Australia, 250 pp.

14. Thapa, K. and Bossler, J. (1992) Accuracy of Spatial Data used in a Geographic Information System,

Photogrammetric Engineering and Remote Sensing, Vol. 58, No. 6, pp. 835-841.

15. Torlegard, K. (1992) Sensors for Photogrammetric Mapping: Review and Prospects, International Society for Photogrammetry and Remote Sensing Journal of Photogrammetry and Remote Sensing, Vol. 47, pp. 241-262.

16. Vlcek, J. (1988) Nature of Video Images, Proceedings of American Society for Photogrammetry and Remote Sensing First Workshop on Videography, Indiana, USA, October, pp. 5-12.

17. Warner, W.S. (1989) A Complete Small-format Aerial Photography System for GIS Data Entry, ITC Journal, Vol. 1989-2, pp. 121-129.

18. Warner, W.S. (1990) Accuracy and Small-format Surveys: The Influence of Scale and Object Definition on Photo Measurements, ITC-Journal, No. 1990-1, pp. 24-27.

19. Wright, R. (1993) Airborne Videography: Principles and Practice, Photogrammetric Record, Vol. 14, No. 81, pp. 447-457.